

---

# COMBINING MULTIPLE POST-TRAINING TECHNIQUES TO ACHIEVE MOST EFFICIENT QUANTIZED LLMs

---

A PREPRINT

**Sayeh Sharify**  
*d-Matrix*  
Santa Clara, CA, USA  
sayehs@d-matrix.ai

**Zifei Xu**  
*d-Matrix*  
Santa Clara, CA, USA  
xuzifei@d-matrix.ai

**Wanzin Yazar**  
*d-Matrix*  
Santa Clara, CA, USA  
wyazar@d-matrix.ai

**Xin Wang**  
*d-Matrix*  
Santa Clara, CA, USA  
xwang@d-matrix.ai

May 14, 2024

**ABSTRACT**

Large Language Models (LLMs) have distinguished themselves with outstanding performance in complex language modeling tasks, yet they come with significant computational and storage challenges. This paper explores the potential of quantization to mitigate these challenges. We systematically study the combined application of two well-known post-training techniques, SmoothQuant and GPTQ, and provide a comprehensive analysis of their interactions and implications for advancing LLM quantization. We enhance the versatility of both techniques by enabling quantization to microscaling (MX) formats, expanding their applicability beyond their initial fixed-point format targets. We show that by applying GPTQ and SmoothQuant, and employing MX formats for quantizing models, we can achieve a significant reduction in the size of OPT models by up to  $4\times$  and LLaMA models by up to  $3\times$  with a negligible perplexity increase of 1–3%.

**Keywords** Microscaling Formats (MX), LLM Quantization, PTQ, GPTQ, SmoothQuant

**1 Introduction**

Large Language Models (LLMs) have emerged as extremely powerful tools to comprehend and generate natural language. However, their intensive computational demand and energy consumption make widespread adoption of these models in everyday tasks to be challenging. One way to address these challenges is post-training quantization, a technique that involves reducing the precision of model parameters and/or activations from the original bit-width to formats with fewer bits. Quantization can significantly reduce the memory footprint and computational requirements of these models, making them more

accessible and deployable on a wider range of hardware, including mobile devices and edge devices. However, previous work has shown that the activations of LLMs with more than 3B parameters are difficult to quantize due to the emergence of outliers with large magnitude, which leads to significant quantization errors and accuracy degradation [1]. To address this issue, Xiao et al. proposed SmoothQuant, a post-training quantization technique that smooths out the activation outliers by migrating the quantization difficulty from activations to weights with a mathematically equivalent transformation [2]. Similarly, Frantar et al. proposed GPTQ, a scalable one-shot quantization method that utilizes approximate second-order information to quantize weights of LLMs with high efficiency and accuracy [3].

To explore the quantization challenges in LLMs, we first examine the difficulty of activation quantization for LLMs by measuring the activation magnitude in a linear layer of DistilGPT2 [4], and demonstrate the presence of outliers across the activations, similar to the LLM.int8() work [1]. Then we systematically study the interaction between two widely adopted LLM quantization techniques, SmoothQuant and GPTQ, which have demonstrated excellent results in quantizing LLMs to the fixed-point formats [2, 3]. Furthermore, we enhance these two algorithms to support quantization to *microscaling* (MX) data formats [5, 6]. We assess the necessity of enabling SmoothQuant for matrix multiplications between activations and weights, as well as those between activations<sup>1</sup>. Finally, we analyze the effect of different quantization granularities (per-channel vs. per-tensor) and quantization ranges (symmetric vs. affine) for fixed-point quantization with SmoothQuant.

---

<sup>1</sup>In the transformer architecture, there are two matrix multiplications between activations: query state with the transpose of key state, and attention score with value state.

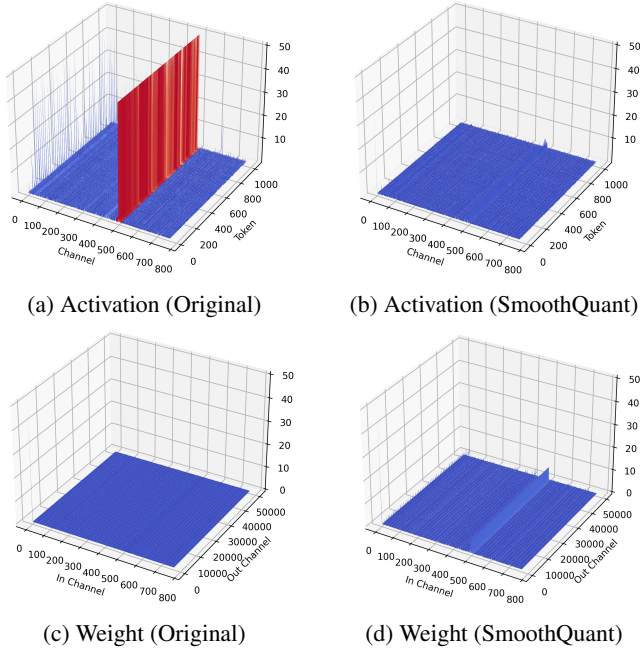


Figure 1: Magnitude of the input activations and weights of the “lm-head” linear layer in DistilGPT2 before and after SmoothQuant. (a) There are a few outlier channels in the original activation tensor. (c) The weight tensor has a flat and uniform distribution. (b and d) By migrating the quantization difficulty from activations to weights we can greatly smooth activation outliers, while still maintaining an easy-to-quantize weight tensor.

**Microscaling format.** The microscaling (MX) format for deep neural net computation was proposed by prior work, first as MSFP [7, 5] and later subsumed by an emerging industry standard *microscaling formats* [6]. Specifically MXINT8, a microscaling format that enables high-accuracy inference using half the memory footprint and twice the throughput of FP16, is an emerging industry standard endorsed by Microsoft, AMD, Arm, Intel, Meta, NVIDIA, and Qualcomm [6], already seeing adoption in today’s hardware products, such as Qualcomm Cloud AI100 Accelerator [8].

The MX format, as outlined in this paper, is characterized by three key components: 1) the scale factor data type, 2) the data type and precision of individual elements, and 3) the scaling block size. The scale factor is applied uniformly across a block of individual elements. This paper specifically focuses on MX formats employing the *INT* data type for individual elements, thus termed *MXINT*.

**Notation.** Throughout the paper we denote a microscaling (MX) format with scaling block size of  $b$ ,  $8$ -bit shared scaling factor, and  $d$  bits per element by *MXINT* $d$ - $b$ . For example, *MXINT6-64* represents an MX format with 6 bits per element, 8 bits shared exponent across 64 values within a block. Unless specified otherwise, for a given tensor the blocking dimension is the last dimension of the tensor. Similarly, a fixed-point value with  $i$  integer bits and no fractional bits is denoted by *INT*- $i$ .

## Contributions:

1. We enhance SmoothQuant and GPTQ to support quantization to microscaling (MX) data formats, extending their compatibility beyond the initially targeted fixed-point formats in the proposed methods.
2. We examine the necessity of enabling SmoothQuant for matrix multiplications between activations and weights, and those between activations. We show that enabling SmoothQuant only for the former operations is sufficient to preserve the perplexity of the baseline models.
3. We study the interaction of SmoothQuant and GPTQ and show that SmoothQuant and GPTQ are synergistic, an effect most prominent in smaller models.

## 2 Activation Quantization Difficulty

Previous work has shown that LLMs are difficult to quantize due to the presence of activation outliers [1, 9, 10]. We verify this by visualizing the input activations and the weights of a linear layer in DistilGPT2 [4]. Figure 1a illustrates the magnitude of the input activations for the “lm-head” layer of DistilGPT2. The existing activation outliers in some of the channels dominate the maximum magnitude measurement, leading to few effective bits for non-outlier values using the per-tensor quantization scheme. This makes it difficult to quantize the activation tensor. On the other hand, as shown in Figure 1c the weight distribution of the same layer is quite uniform and flat, making its quantization easier compared to quantizing the activations. SmoothQuant proposes a technique to migrate the quantization difficulty from activations to weights, such that the “smoothed” activations and the adjusted weights are both easy to quantize [2].

## 3 SmoothQuant

SmoothQuant (SQ) is a quantization method that targets both activations and weights of a model [2]. In this approach, the activation of a linear layer is scaled by a per-channel smoothing factor  $s \in R^{C_i}$  to minimize quantization errors. Simultaneously, the weight of the layer is adjusted in the opposite direction to maintain the mathematical equivalence of the linear layer:

$$\mathbf{Y} = (\mathbf{X}\text{diag}(s)^{-1}) \cdot (\text{diag}(s)\mathbf{W}) = \hat{\mathbf{X}}\hat{\mathbf{W}} \quad (1)$$

In Equation 1,  $\mathbf{X}$  is the original input activation with outliers, and  $\hat{\mathbf{X}} = \mathbf{X}\text{diag}(s)^{-1}$  is the smoothed activation. To minimize the quantization error of the input activation, the smoothing factor is selected such that all channels of the smoothed input activation have the same maximum magnitude. Accordingly,  $s$  is set to:

$$s_j = \max(|\mathbf{X}_j|), \quad j = 1, 2, \dots, C_i \quad (2)$$

Where  $C_i$  is the number of input channels in the input activation and  $j$  corresponds to  $j^{\text{th}}$  input channel. Note that since the range of activations varies for different input samples, the

**Algorithm 1** Enhanced GPTQ: Quantize  $\mathbf{W}$  given inverse Hessian  $\mathbf{H}^{-1} = (2\mathbf{X}\mathbf{X}^T + \lambda\mathbf{I})^{-1}$ , block size  $B_1$ , and micro-block size  $B_2$ .

---

**Input:**  $\mathbf{W}$  // Weight matrix  
**Input:**  $d_{row}$  // Row dimension of  $\mathbf{W}$   
**Input:**  $d_{col}$  // Column dimension of  $\mathbf{W}$   
**Input:**  $B_1$  // Block size  
**Input:**  $B_2$  // Micro-block size  
**Input:**  $\mathbf{H}^{-1}$  // Hessian inverse information  
**Variable:**  $E$  // Quantization error matrix  
**Output:**  $\mathbf{Q}$  // Quantized weight matrix  
**Initialize:**  $\mathbf{Q} \leftarrow 0_{d_{row} \times d_{col}}$   
**Initialize:**  $E \leftarrow 0_{d_{row} \times d_{col}}$   
**Initialize:**  $\mathbf{H}^{-1} \leftarrow \text{Cholesky}(\mathbf{H}^{-1})^T$   
**for**  $i = 0, B_1, 2B_1, \dots$  **do**  
  **for**  $j = i, i + B_2, i + 2B_2, \dots, i + B_1 - 1$  **do**  
     $k \leftarrow j + B_2$  // helper index  
     $\mathbf{Q}_{:,j:k} \leftarrow \text{quant}(\mathbf{W}_{:,j:k})$   
     $\mathbf{E}_{:,j:k} \leftarrow (\mathbf{W}_{:,j:k} - \mathbf{Q}_{:,j:k})([\mathbf{H}^{-1}]_{j:k,j:k})^{-1}$   
     $\mathbf{W}_{:,k} \leftarrow \mathbf{W}_{:,k} - \mathbf{E}_{:,j:k}[\mathbf{H}^{-1}]_{j:k,k}$   
  **end for**  
   $\mathbf{W}_{:,i+B_1} \leftarrow \mathbf{W}_{:,i+B_1} - \mathbf{E}_{:,i:i+B_1}[\mathbf{H}^{-1}]_{i:i+B_1,i+B_1}$   
**end for**  
**Return:**  $\mathbf{Q}$

---

maximum value of each channel is estimated using 128 calibration samples from the calibration dataset (see Section 5.1 for more details). By dividing the input activation by the the scaling factor of Equation 2, all channels of the scaled input activation would have the same range, making quantization of the scaled tensor to be very easy. However, this will migrate the difficulty of the quantization completely to the weight side of a linear layer. To address this issue, Xiao et al. proposed a scaling formula that balances the quantization difficulty of activations and weights:

$$s_j = \max(|\mathbf{X}_j|)^\alpha / \max(|\mathbf{W}_j|)^{1-\alpha}, \quad j = 1, 2, \dots, C_i \quad (3)$$

Where  $\alpha$  is a hyper-parameter that controls how much quantization difficulty we want to migrate from activations to weights. For quantization to the MX format using SmoothQuant, we directly calculated the SmoothQuant scaling factors, skipping the additional calibration phase required for quantization to fixed-point formats. For more details on the SmoothQuant algorithm refer to Xiao et al.’s work [2].

## 4 GPTQ

GPTQ is a post-training quantization (PTQ) method that uses second-order Hessian information for weight quantization in LLMs [3]. It employs layer-wise quantization for each layer  $l$  in the network, seeking quantized weights  $\hat{\mathbf{W}}_l$  that make the outputs ( $\hat{\mathbf{W}}_l \mathbf{X}_l$ ) closely approximate those of the original weights ( $\mathbf{W}_l \mathbf{X}_l$ ). In other words, GPTQ aims to find [3]:

$$\text{argmin}_{\hat{\mathbf{W}}_l} \|\mathbf{W}_l \mathbf{X}_l - \hat{\mathbf{W}}_l \mathbf{X}_l\|_2^2 \quad (4)$$

To solve equation 4, GPTQ quantizes each row of the weight matrix,  $\mathbf{W}$ , independently, focusing on a single weight per row

at a time. It consistently updates all not-yet-quantized weights to offset the error introduced by quantizing a single weight. Since the objective function in equation 4 is quadratic, its Hessian  $\mathbf{H}$  can be calculated using the following formula, where  $F$  denotes the set of remaining full-precision weights:

$$\mathbf{H}_F = 2\mathbf{X}_F \mathbf{X}_F^T \quad (5)$$

Given  $\mathbf{H}$ , the next to be quantized weight,  $w_q$ , and the corresponding update of all remaining weights in  $F$ ,  $\delta_F$ , are given by the following formulas, where  $\text{quant}(w)$  rounds  $w$  to the nearest quantized value [3]:

$$w_q = \text{argmin}_{w_q} \frac{(w_q - \text{quant}(w_q))^2}{[\mathbf{H}_F^{-1}]_{qq}} \quad (6)$$

$$\delta_q = -\frac{w_q - \text{quant}(w_q)}{[\mathbf{H}_F^{-1}]_{qq}} \cdot (\mathbf{H}_F^{-1})_{:,q}$$

For all rows of  $\mathbf{W}$ , GPTQ quantizes weights in the same order. This accelerates the process, as certain computations need to be performed only once for each column rather than once for each weight. Additionally, the vectorized implementation of GPTQ enables processing multiple rows of  $\mathbf{W}$  simultaneously.

The GPTQ algorithm, as originally proposed, is designed for quantization to a fixed-point format. We have enhanced the algorithm to also support quantization to a *microscaling (MX) format*. Algorithm 1 provides pseudocode for the modified GPTQ, that enables MX quantization. Note that for quantizing  $\mathbf{W}$  to a specific MX format, the micro-block size in the algorithm,  $B_2$ , should be a multiple of the block size of the MX format. Additionally, to reduce the GPU memory requirement, we have implemented the GPTQ quantization process on the actual layer inputs in the partially quantized model rather than on the layer inputs of the full precision model. For more details on the GPTQ algorithm refer to Frantar et al.’s work [3].

## 5 Experiments

### 5.1 Setups

**Models.** We benchmarked different quantization methods on DistilGPT2 [4], the OPT [11], and the LLaMA [12] families. DistilGPT2 is a distilled version of GPT-2 with only 82 million parameters. It is challenging to quantize a parameter-efficient model like DistilGPT2 as the model is already designed to be compact, and further reducing precision during quantization may hurt the model performance significantly, requiring careful optimization to maintain the desired balance between model size and accuracy. LLaMA and OPT are two families of open-source LLMs that are widely accepted among the machine learning community due to their superior performance compared to other open-source LLMs [1, 3, 2, 13]. LLaMA is also considered to be the foundation of many popular open-source models such as Alpaca [14], Vicuna [15], Guanaco [16], and Stable Beluga [17].

**Datasets.** Following previous work [1, 2, 3, 13, 18, 19], we measured the perplexity of quantized language models on *WikiText-2* [20] as perplexity can stably reflect the performance of LLMs [18, 13]. Unless otherwise stated, the *test* split of the dataset is used to evaluate the models.

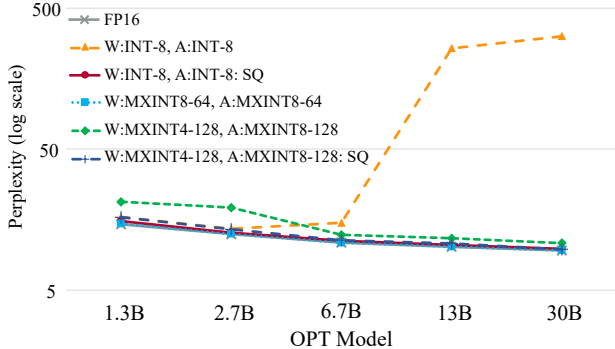


Figure 2: Perplexity for OPT models with different sizes when quantized to INT-8, MXINT8-64, and MXINT4-128. The Y-axis represents perplexity in logarithmic scale. The X-axis represents the OPT models with different sizes. The *Per-tensor affine* scheme is used for INT-8 quantization of both activations and weights. The figure shows that: a) For models larger than 6.7B parameters quantization to INT-8 significantly degrades model performance, this is shown by a cliff in the perplexity curve of INT-8 at 6.7B (the orange curve). b) There are no such cliffs with the MXINT quantizations. c) SmoothQuant mitigates the cliff, preserving the baseline (FP16) perplexity of OPT models across different scales when quantized to INT-8. d) SmoothQuant is beneficial with more aggressive quantization to MXINT4, reducing the perplexity gap between the baseline model and the quantized models.

**Quantization formats.** We evaluated models using different microscaling and fixed-point quantization formats; the same numerical format was applied for quantizing both activations and weights unless specified otherwise. For the fixed-point quantization, we calibrated the models using 128 random input sentences from *WikiText-2-train* to estimate the dynamic range of activations. We utilized *MinMaxObserver* to find the range of activations, and calculated the zero-point and the scale parameters for the activations and weights in per-tensor granularity levels.

**Activation smoothing.** We calculated the per-channel scaling factor for activations and weights using the formula stated in Equation 1. As in the previous work, we consistently use a migration strength ( $\alpha$ ) value of 0.5 across all models throughout the paper. To calculate the scaling factors, we gathered the statistics of activations using 128 random sentences from the *WikiText-2-train* dataset. Once we calculated the scaling factors, we used the same values to evaluate the models with different quantization formats.

**Targeted layers.** Similar to the previous work [2], we apply smoothing on the input activation of the self-attention and the feed-forward layers of LLMs. Unless stated otherwise, we transform all *Linear* layers, *HFCnvID* layers, and *Activation* by *Activation* matrix multiplications to the specified quantization format while keeping the activation/weight in the original format for other layers including *ReLU*, *GELU*, *Softmax*, and *LayerNorm*.

Table 1: DistilGPT2 quantization results, with and without SmoothQuant. Act, Wgt, and PPL denote activation, weight, and perplexity, respectively.  $\downarrow$ : the lower the metric, the better the result. We used *per-tensor affine* quantization for the fixed-point formats. LR: Likelihood Ratio over SmoothQuant disabled.

Act & Wgt format	$\downarrow$ PPL w/o SQ	$\downarrow$ PPL w/ SQ	LR
Baseline (FP32)	<b>46.06</b>	N/A	N/A
MXINT16-64	<b>46.06</b>	<b>46.06</b>	1.00
MXINT16-32	<b>46.06</b>	<b>46.06</b>	1.00
INT-8	59.23	60.91	0.97
MXINT8-128	46.49	46.27	1.00
MXINT8-16	46.22	<b>46.10</b>	1.00
INT-6	2230.21	1875.86	1.19
MXINT6-128	54.09	51.91	1.04
MXINT6-16	48.42	<b>47.70</b>	1.02
INT-4	11559.05	7367.77	1.57
MXINT4-128	1649.68	898.35	1.84
MXINT4-16	153.87	<b>123.53</b>	1.25

## 5.2 Results

### 5.2.1 SmoothQuant effect on quantization

In this section, we evaluate the impact of the SmoothQuant technique on the quantization of LLMs from different families: OPT, DistilGPT2, LLaMA, and the llama2 models. We employ various fixed-point and MX formats with different bit-widths for our assessment.

**OPT family.** To explore the impact of SmoothQuant on the quantization of the OPT family [11], first we reproduce the observation of the *INT-8 quantization cliff phenomenon* without applying SmoothQuant [1, 21]. We measure the perplexity of OPT models with different sizes when quantized to INT-8 and show that with scaling up the model size beyond 6.7B parameters, performance of the quantized model catastrophically degrades. This is shown with a cliff in perplexity at the 6.7B point of the orange curve (Figure 2). We further verify that introducing SmoothQuant rectified this anomaly, resulting in perplexities monotonically decreasing with increasing model size [2].

Next, we ask *whether quantization to MX formats, e.g., MX-INT8 and MXINT4, results in a similar quantization cliff anomaly?* To answer this question, we quantize the same models to the MXINT8 and the MXINT4 formats and show that quantization of the models to either of these formats does not result in a similar anomaly; see Figure 2. Moreover, we demonstrate that across different model sizes, quantization to MXINT8 maintains the model perplexity while more aggressive quantization to MXINT4 penalizes perplexity by 13-44%. Enabling SmoothQuant improves performance of the MXINT4 models narrowing the perplexity gap between the baseline models and the quantized models to 1-12%. Table 6 in the appendix section indicates the detailed quantization results for the OPT family.

Table 2: Quantization results for the LLaMA models with different sizes on *WikiText-2-test*, with and without SmoothQuant. Act, Wgt, SQ, and PPL denote activation, weight, SmoothQuant, and perplexity, respectively. ↓: the lower the metric, the better the result. We used *per-tensor affine* quantization for the fixed-point formats. LR: Likelihood Ratio of perplexity with SmoothQuant enabled over perplexity with SmoothQuant disabled.

Model	LLaMA-7B			LLaMA-13B			LLaMA-30B		
	↓PPL w/o SQ	↓PPL w/ SQ	LR	↓PPL w/o SQ	↓PPL w/ SQ	LR	↓PPL w/o SQ	↓PPL w/ SQ	LR
Baseline (FP16)	<b>5.67</b>	N/A	N/A	<b>5.09</b>	N/A	N/A	<b>4.10</b>	N/A	N/A
MXINT16-64	<b>5.67</b>	<b>5.67</b>	1.00	<b>5.09</b>	<b>5.09</b>	1.00	<b>4.10</b>	<b>4.10</b>	1.00
MXINT16-32	<b>5.67</b>	<b>5.67</b>	1.00	<b>5.09</b>	<b>5.09</b>	1.00	<b>4.10</b>	<b>4.10</b>	1.00
INT-8	19.01	19.19	0.99	28.90	43.72	0.66	17.72	19.88	0.89
MXINT8-128	<b>5.68</b>	5.69	1.00	5.10	<b>5.09</b>	1.00	4.11	4.11	1.00
MXINT8-16	<b>5.68</b>	<b>5.68</b>	1.00	<b>5.09</b>	<b>5.09</b>	1.00	<b>4.10</b>	<b>4.10</b>	1.00
INT-6	45202.57	58760.27	0.77	65911.20	42067.46	1.56	27764.73	31869.35	0.87
MXINT6-128	5.83	5.83	1.00	5.20	5.17	1.00	4.29	4.24	1.01
MXINT6-16	<b>5.72</b>	<b>5.72</b>	1.00	<b>5.12</b>	<b>5.12</b>	1.00	4.17	<b>4.14</b>	1.01
INT-4	185803.03	230625.14	0.81	158380.31	160879.97	0.98	152000.44	173788.06	0.87
MXINT4-128	16.35	12.87	1.27	11.69	9.60	1.22	10.49	8.06	1.30
MXINT4-16	7.43	<b>7.12</b>	1.04	6.22	<b>6.05</b>	1.03	5.66	<b>5.22</b>	1.08

**DistilGPT2.** Table 1 illustrates quantization results for DistilGPT2 with and without SmoothQuant using different quantization formats. We found that generally, aggressive quantization to fewer bits increases perplexity for both the fixed-point and the MX formats. However, for a given bit-width, using MX results in better perplexity compared to the fixed-point format. Remarkably, for almost all of the studied quantization bit-widths and formats, enabling SmoothQuant increases the quantization quality, leading to better perplexity. The advantage of enabling SmoothQuant is small with larger precisions. Under more restrictive bit-widths and larger block sizes, SmoothQuant becomes more advantageous.

**LLaMA family.** Table 2 illustrates perplexity of the quantized LLaMA models [12] with three different sizes on WikiText-2-test using various MX and fixed-point formats. For all three models, aggressive quantization to small bit-widths significantly hurts the model performance, while quantizing to higher bit-widths has negligible effect on perplexity. For example, quantizing LLaMA-7B to MXINT16 preserves the baseline perplexity of the model regardless of the format block size, while quantizing to MXINT4-16 increases perplexity by 31% to 7.43. Moreover, quantization results using different MX format delivers better perplexity compared to the fixed-point formats with the same bit-width. For instance, quantizing LLaMA-13B to INT-6 significantly increases perplexity to 65911, enabling SmoothQuant reduces it to 42067 which is still far from the baseline perplexity of 5.09, while using MXINT6-16 and enabling SmoothQuant we can achieve perplexity of 5.12. Additionally, for all three models, across MXINT formats with same precision, enabling SmoothQuant is more advantageous when quantizing to formats with larger block sizes compared to the formats with smaller block sizes. For example, when quantizing LLaMA-13B to MXINT4-128 enabling SmoothQuant improves the model perplexity by 22% while with quantizing to MXINT4-16, enabling SmoothQuant only reduces the perplexity by 3%. Finally, for the studied models regardless of the quantization format and precision, the advantage of enabling SmoothQuant is marginal with larger

models and higher quantization precisions and is especially prominent for smaller models with more restrictive bit-widths.

Similarly, we assess the impact of SmoothQuant on the quantization of the llama2 family [22] using various fixed-point and MX formats with different precisions. We observe similar trends to those identified in the LLaMA study. Detailed results of the experiment can be found in the Table 7 of the appendix.

### 5.2.2 Activation by Activation SmoothQuant

The previous work [2] enabled SmoothQuant for the input activations of all of the matrix multiplications for a given model, regardless of the type of their operands. In this section, we divide the multiplications to two categories based on their operand types, and study the necessity of enabling SmoothQuant for each category separately. The two categories are a) *activation by activation* multiplications which includes  $Query \times Key\text{-transpose}$  and  $Activation\text{-probability} \times Value$  operations of the self-attention blocks, and b) *activation by weight* multiplications which covers all *Linear* and *HFCConv1D* layers of the networks. We refer to the former as *A-A SmoothQuant*, and the latter as *A-W SmoothQuant*, in the rest of the manuscript. In the aforementioned studies where SmoothQuant significantly improved the performance of the quantized models, we ask whether the improvement was due to *A-W* or to *A-A SmoothQuant*, or their combination?

To answer this question, we performed ablation studies on the two types of SmoothQuant, on three models from three different LLM families: DistilGPT2, OPT-6.7B, and LLaMA-7B evaluated on WikiText-2-test (Table 3). We found that for all three networks, A-W SmoothQuant is sufficient to lead to the observed accuracy improvement, and A-A SmoothQuant does not contribute to the improvement materially. Additionally, contrary to previous research [2], we found that further enabling A-A SmoothQuant on top of A-W SmoothQuant significantly degrades the performance of LLaMA-7B by 10% when quantized to INT-8.

Table 3: Perplexity of the quantized models for DistilGPT2, OPT-6.7B, and LLaMA-7B on *WikiText-2-test*. For INT-8 quantization of activations and weights the *per-tensor affine* scheme is used. Act, Wgt, SQ, and PPL denote activation, weight, SmoothQuant, and perplexity, respectively. ↓: the lower the metric, the better the result. For all three models, only enabling A-W SmoothQuant is sufficient to reduce perplexity of the quantized models.

Act & Wgt format		A:INT-8 W:INT-8	A:MXINT8 W:MXINT8	A:MXINT8 W:MXINT4
A-A SQ	A-W SQ	DistilGPT2 ↓PPL (FP32 PPL: 46.06)		
disabled	disabled	<b>59.23</b>	46.37	72.97
disabled	enabled	60.57	<b>46.23</b>	<b>72.93</b>
enabled	disabled	59.90	46.35	77.18
enabled	enabled	60.91	<b>46.23</b>	77.24
A-A SQ	A-W SQ	OPT-6.7B ↓PPL (FP16 PPL: 10.86)		
disabled	disabled	15.01	<b>10.86</b>	12.33
disabled	enabled	<b>11.10</b>	<b>10.86</b>	11.30
enabled	disabled	15.01	<b>10.86</b>	12.35
enabled	enabled	11.17	<b>10.86</b>	<b>11.29</b>
A-A SQ	A-W SQ	LLaMA-7B ↓PPL (FP16 PPL: 5.67)		
disabled	disabled	19.01	<b>5.68</b>	6.31
disabled	enabled	<b>17.47</b>	<b>5.68</b>	<b>6.18</b>
enabled	disabled	19.40	<b>5.68</b>	6.31
enabled	enabled	19.19	<b>5.68</b>	<b>6.18</b>

### 5.2.3 SmoothQuant with different fixed-point quantization schemes

In this section, we study the effect of different *quantization granularity* (*per-tensor* vs *per-channel*) and *quantization range* (*symmetric* vs *affine*) for fixed-point quantization, with and without enabling SmoothQuant.

**Quantization granularity.** Quantization can be done in different granularities. The *per-tensor* quantization uses a single scale and zero-point values to quantize the entire tensor while the *per-channel* quantization enables finer-grained quantization by using different scales and zero-point parameters for values associated with each channel of a given tensor.

**Quantization range.** Quantization can have a symmetric or asymmetric range. In *symmetric* quantization we assume that the given tensor has the same negative and positive ranges and is symmetric around 0, while in *affine* quantization a *zero-point* offset is used to shift the quantization levels according to the negative and positive ranges of the given tensor.

Table 4 reports quantization perplexity for DistilGPT2 on *WikiText-2-test* with different calibration techniques enabling and disabling SmoothQuant. Calibration is done using 128 random input sentences from *WikiText-2-train*. The INT-8 quantization format is used for both activation and weights. Based on the results of Section 5.2.2, with INT-8 quantization only enabling A-W SmoothQuant provides smaller perplexity numbers compared to enabling both A-A SmoothQuant and A-W SmoothQuant. Thus, in this study only the latter is enabled. We found that: a) generally the *affine* calibration method results in better perplexity compared to its corresponding *symmetric* technique regardless of enabling or

Table 4: Perplexity for *DistilGPT2*, *OPT-6.7B*, and *LLaMA-7B* on *WikiText-2-test* with different quantization schemes. Act, Wgt, SQ, PPL, and Quant. denote activation, weight, SmoothQuant, perplexity, and Quantization, respectively. Both activations and weights are quantized to INT-8. Enabling A-W SmoothQuant is only beneficial for *per-tensor affine* calibrations. ↓: The lower the metric, the better the result.

Act & Wgt format		INT-8	
↓PPL w/o & w/ A-W SmoothQuant		w/o SQ	w/ SQ
Quant. granularity		DistilGPT2	
per-tensor	symmetric	92.91	228.26
per-tensor	affine	59.23	60.57
per-channel	symmetric	54.08	54.32
per-channel	affine	<b>48.13</b>	48.33
Quant. granularity		OPT-6.7B	
per-tensor	symmetric	93.19	13222.79
per-tensor	affine	15.01	11.10
per-channel	symmetric	12.91	13.17
per-channel	affine	<b>10.96</b>	11.09
Quant. granularity		LLaMA-7B	
per-tensor	symmetric	38.51	23.89
per-tensor	affine	19.01	17.38
per-channel	symmetric	6.63	6.64
per-channel	affine	5.93	<b>5.92</b>

disabling SmoothQuant; b) for *per-tensor affine* calibrations, enabling SmoothQuant improves quantization results significantly c) in most cases, with *per-channel* calibrations, enabling SmoothQuant slightly degrades perplexity; accordingly, SmoothQuant is not required with the *per-channel* calibration scheme.

### 5.2.4 SmoothQuant and GPTQ Interaction

GPTQ has been shown to improve quality of models whose weights are quantized to lower than 8-bit integer formats [3]. Since we know from the above results that SmoothQuant also improves model accuracies in these modes, a natural question arises: *how do SmoothQuant and GPTQ interact when they are applied jointly?*

To answer this question, we conduct experiments on quantization of the OPT, and the LLaMA families where SmoothQuant and GPTQ are applied individually, as well as jointly to assess their impact on the quantization quality. As shown in Section 5.2.1, for both the OPT and LLaMA models quantization to *MXINT8* maintains the model perplexity across different model sizes, thus there is no need to enable SmoothQuant or GPTQ with *MXINT8* quantization. Accordingly, in this section we have considered the joint application of SmoothQuant and GPTQ only for quantization to *MXINT4*, and *INT-8*. Moreover, we showed that SmoothQuant is only beneficial with the *per-tensor affine* scheme (Section 5.2.3). Thus, in this section for *INT-8* quantization of activations and weights this method is used.

Table 5 illustrates our experiment results for the OPT family. We found that for large models with more than 6.7B parameters, enabling SmoothQuant is essential to preserve the per-



Table 5: Quantization results for the OPT models with different sizes on *WikiText-2-test*, with enabling/disabling GPTQ and A-W SmoothQuant. A, W, SQ, and PPL denote activation, weight, SmoothQuant, and perplexity, respectively.  $\downarrow$ : the lower the metric, the better the result. We used *per-tensor affine* quantization for the INT-8 format.

Act & Wgt format		A:INT-8 W:INT-8	A:MXINT8 W:MXINT4
GPTQ SQ		OPT-125M (FP16 $\downarrow$ PPL: 27.66)	
disabled	disabled	37.75	39.52
disabled	enabled	36.13	35.86
enabled	disabled	36.97	33.63
enabled	enabled	<b>35.36</b>	<b>31.66</b>
GPTQ SQ		OPT-1.3B (FP16 $\downarrow$ PPL: 14.63)	
disabled	disabled	16.43	18.94
disabled	enabled	15.44	16.16
enabled	disabled	16.40	18.00
enabled	enabled	<b>15.41</b>	<b>15.52</b>
GPTQ SQ		OPT-6.7B (FP16 $\downarrow$ PPL: 10.86)	
disabled	disabled	14.92	12.19
disabled	enabled	<b>11.09</b>	11.20
enabled	disabled	14.73	11.12
enabled	enabled	<b>11.09</b>	<b>11.03</b>
GPTQ SQ		OPT-13B (FP16 $\downarrow$ PPL: 10.12)	
disabled	disabled	255.85	11.52
disabled	enabled	11.03	10.54
enabled	disabled	250.77	<b>10.28</b>
enabled	enabled	<b>10.98</b>	10.31

plexity of the baseline model, when quantizing to *INT-8*, and applying *GPTQ* on top of SmoothQuant only improves the performance of the quantized models slightly. With *MX* quantization, the advantageous of jointly enabling SmoothQuant and GPTQ over only applying SmoothQuant is small for large models. This becomes more advantageous with smaller models. For instance, perplexity of *OPT-125M* when quantized to *MXINT4* is 39.52. Enabling SmoothQuant improves the performance of the quantized model reducing its perplexity by 9% to 35.86 and applying GPTQ, decreases perplexity by another 12% to 31.66. While with *MX* quantization of *OPT-13B*, further enabling GPTQ on top of SmoothQuant only reduces perplexity by 2% from 10.54 to 10.31.

We conducted a similar experiment with DistilGPT2, the LLaMA, and the llama2 families. In contrast to the findings from the OPT study, for these cases, the best results were achieved, except when quantizing llama2-13B to INT-8, with only applying GPTQ. However, for the INT-8 quantization of llama2-13B, SmoothQuant proved to be the solution to improve the perplexity degradation of the quantized model. Additional details on these experiments can be found in the appendix (Tables 8 and 9).

### 5.2.5 Pareto frontier Study

The objective of a quantization method is to reduce the model size while preserving its accuracy. In the experiments conducted in this study, the concept of the *Pareto frontier* becomes relevant in determining the most suitable quantization method

for each model under a size constraint. A model is deemed to be on the Pareto frontier if no other model exists with both a smaller size and lower perplexity. Figure 3 illustrates perplexity of the LLaMA and llama2 families on WikiText-2-test as a function of model parameter size. Points corresponding to the quantized models on Pareto frontiers are marked with a gray circle. We observe that, in general, for aggressive weight quantization to 4-bit (e.g., MXINT4), models quantized with GPTQ are positioned on Pareto frontiers while in the case of quantization to 6-bit (e.g., MXINT6), models quantized with SmoothQuant are found on Pareto frontiers. Lastly, for a more relaxed quantization to 8-bit (e.g., MXINT8), neither GPTQ nor SmoothQuant is deemed necessary.

Additionally, we explored Pareto frontiers for the OPT family revealing similar trends to those observed for the LLaMA and llama2 families. However, for the quantization of small OPT models to MXINT4 (e.g., OPT-1.3B and OPT-6.7B), the best perplexity is achieved when both GPTQ and SQ are applied jointly. Further details on the Pareto frontiers study of the OPT family can be found in Figure 4 in the appendix. Note that in none of the aforementioned studies, no fixed-point quantization points appear on the Pareto frontiers, indicating that, for the studied models and quantization ranges, the MX format is more suitable for quantizing the models compared to the fixed-point format with the same bit-width. Moreover, we studied the effects of block size granularity on quantization to microscaling and fixed-point formats, and found that regardless of the quantization granularity for quantization to 6-bit and 8-bit, the majority of points on the Pareto frontier are associated with MX data-types, more details is presented in Section A.4 of appendix.

## 6 Related Work

**Model quantization methods.** Quantization is a technique that lowers the bit precision of deep learning models, effectively reducing model size and accelerating inference. There are two primary categories of quantization techniques: Quantization-Aware Training (QAT), which leverages back-propagation to update quantized weights [23, 24, 25, 26], and Post-Training Quantization (PTQ), which typically requires no additional training. Quantization-aware training methods cannot easily scale up to quantize giant LLMs. Consequently, PTQ methods are commonly employed for quantizing LLMs [27, 28, 29, 30, 31, 32, 33]. In this work, we studied the interaction of two PTQ methods, GPTQ [3] and SmoothQuant [2].

**Large Language Model quantization.** With the recent open-source releases of language models like OPT [11] and LLaMA [12], researchers are actively working on developing cost-effective methods to compress these large networks for inference. Various approaches have been suggested to tackle the challenges of quantizing LLMs. ZeroQuant [19] and nuQmm [34] employ per-token and group-wise quantization schemes for LLMs, requiring customized CUDA kernels. ZeroQuant further proposes layer-wise knowledge distillation, similar to AdaQuant [31], but the largest evaluated model by both ZeroQuant and nuQmm has 20B parameters.

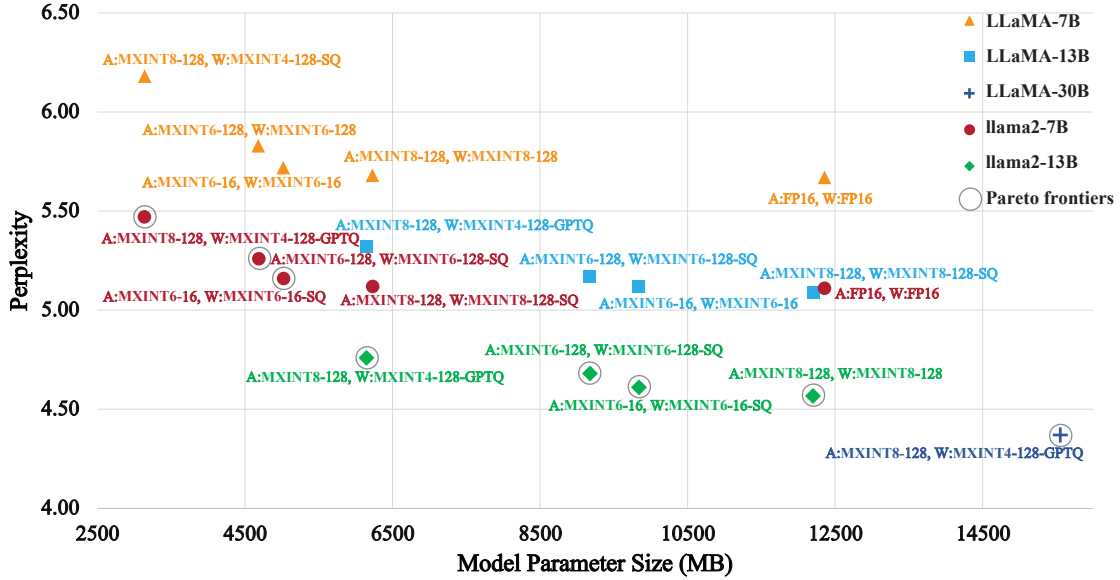


Figure 3: Perplexity for the LLaMA and llama2 families when quantized to MXINT8, and MXINT4. The Y-axis represents perplexity. The X-axis represents model parameter size including the additional scale parameters required by the SmoothQuant quantization method. Note that the GPTQ algorithm does not introduce any additional model parameters during the inference. A, W, and SQ denote activation, weight, and SmoothQuant. The points corresponding to the quantized models on Pareto frontiers are indicated by a gray circle.

LLM.int8() identifies activation outliers in a few feature dimensions as a hindrance to the quantization of larger models. To address this issue, it proposes to preserve those dimensions in higher precision using a mixed INT8/FP16 decomposition [1]. However, this implementation results in significant latency overhead, sometimes even slower than FP16 inference. Similarly, SpQR [35] and OWQ [36] propose to retain outlier features that are difficult to quantize in full-precision, while AWQ [13] mitigates the quantization error for the outliers using grid-searched channel-wise scaling. Additionally, Outlier Suppression [9] tackles activation outliers by utilizing non-scaling LayerNorm and token-wise clipping. Despite its success with smaller language models such as BERT [37] and BART [38], it falls short in maintaining accuracy for larger LLMs, while SmoothQuant and GPTQ both preserve the performance of LLMs up to 175B parameters [2, 3]. Lee et al., explored the combined use of GPTQ and SmoothQuant for quantizing LLMs, focusing solely on fixed-point data types in their study [39]. Trukhanov et al., proposed a technique for quantizing KV-cache to low-precision Block Floating-Point (BFP) formats without compromising the resulting model accuracy [40].

## 7 Conclusion

To summarize, our study showed that the optimality of decisions on whether to combine the GPTQ and the SmoothQuant techniques depends on factors such as numerical precision, data type, model family, and model size. SmoothQuant can be effective for quantizing both activations and weights in large language models using different fixed-point and MX formats. This benefit is particularly pronounced within the quantization

formats ranging from 6 to 8 bits. Conversely, GPTQ demonstrated superior weight effectiveness in scenarios involving more aggressive weight quantization, particularly to 4 bits and 6 bits. Notably, our findings indicated that for quantization to MXINT8, neither GPTQ nor SmoothQuant is necessary to preserve the baseline accuracy. We demonstrated that quantizations using different MX formats deliver better perplexity compared to fixed-point formats with the same bit-width when the per-tensor quantization scheme is employed.

Additionally, contrary to the results of prior research [2], we illustrated that when applying SmoothQuant, it suffices to apply only the A-W SmoothQuant, as opposed to the original findings that recommended both A-W and A-A approaches. Throughout the paper, we have shown that by utilizing GPTQ and A-W SmoothQuant, and quantizing models to MX formats, we can significantly reduce the size of OPT models by up to 4 $\times$  and LLaMA models by up to 3 $\times$  with negligible perplexity degradation.

## References

- [1] T. Dettmers, M. Lewis, Y. Belkada, and L. Zettlemoyer, “Llm.int8(): 8-bit matrix multiplication for transformers at scale,” *arXiv preprint arXiv:2208.07339*, 2022.
- [2] G. Xiao, J. Lin, M. Seznec, H. Wu, J. Demouth, and S. Han, “Smoothquant: Accurate and efficient post-training quantization for large language models,” in *International Conference on Machine Learning*, pp. 38087–38099, PMLR, 2023.



- [3] E. Frantar, S. Ashkboos, T. Hoefler, and D. Alistarh, “GPTQ: Accurate post-training quantization for generative pre-trained transformers,” *arXiv preprint arXiv:2210.17323*, 2022.
- [4] V. Sanh, L. Debut, J. Chaumond, and T. Wolf, “Distilbert, a distilled version of bert: smaller, faster, cheaper and lighter,” in *NeurIPS EMC Workshop*, 2019.
- [5] B. Darvish Rouhani, R. Zhao, V. Elango, R. Shafipour, M. Hall, M. Mesmakhosroshahi, A. More, L. Melnick, M. Golub, G. Varatkar, *et al.*, “With shared microexponents, a little shifting goes a long way,” in *Proceedings of the 50th Annual International Symposium on Computer Architecture*, pp. 1–13, 2023.
- [6] B. D. Rouhani, R. Zhao, A. More, M. Hall, A. Khodamoradi, S. Deng, D. Choudhary, M. Cornea, E. Dellinger, K. Denolf, *et al.*, “Microscaling data formats for deep learning,” *arXiv preprint arXiv:2310.10537*, 2023.
- [7] B. Darvish Rouhani, D. Lo, R. Zhao, M. Liu, J. Fowers, K. Ovtcharov, A. Vinogradsky, S. Massengill, L. Yang, R. Bittner, *et al.*, “Pushing the limits of narrow precision inferencing at cloud scale with microsoft floating point,” *Advances in neural information processing systems*, vol. 33, pp. 10271–10281, 2020.
- [8] Qualcomm, “Qualcomm Cloud AI 100 Accelerator.” <https://www.qualcomm.com/developer/blog/2024/01/qualcomm-cloud-ai-100-accelerates-large-language-model-inference-2x-using-microscaling-mx>, 2023.
- [9] X. Wei, Y. Zhang, X. Zhang, R. Gong, S. Zhang, Q. Zhang, F. Yu, and X. Liu, “Outlier suppression: Pushing the limit of low-bit transformer language models,” *Advances in Neural Information Processing Systems*, vol. 35, pp. 17402–17414, 2022.
- [10] Y. Bondarenko, M. Nagel, and T. Blankevoort, “Understanding and overcoming the challenges of efficient transformer quantization,” *arXiv preprint arXiv:2109.12948*, 2021.
- [11] S. Zhang, S. Roller, N. Goyal, M. Artetxe, M. Chen, S. Chen, C. Dewan, M. Diab, X. Li, X. V. Lin, *et al.*, “OPT: Open pre-trained transformer language models,” *arXiv preprint arXiv:2205.01068*, 2022.
- [12] H. Touvron, T. Lavril, G. Izacard, X. Martinet, M.-A. Lachaux, T. Lacroix, B. Rozière, N. Goyal, E. Hambro, F. Azhar, *et al.*, “LLaMA: Open and efficient foundation language models,” *arXiv preprint arXiv:2302.13971*, 2023.
- [13] J. Lin, J. Tang, H. Tang, S. Yang, X. Dang, and S. Han, “AWQ: Activation-aware weight quantization for llm compression and acceleration,” *arXiv preprint arXiv:2306.00978*, 2023.
- [14] R. Taori, I. Gulrajani, T. Zhang, Y. Dubois, X. Li, C. Guestrin, P. Liang, and T. B. Hashimoto, “Alpaca: A strong, replicable instruction-following model,” *Stanford Center for Research on Foundation Models*. <https://crfm.stanford.edu/2023/03/13/alpaca.html>, vol. 3, no. 6, p. 7, 2023.
- [15] W.-L. Chiang, Z. Li, Z. Lin, Y. Sheng, Z. Wu, H. Zhang, L. Zheng, S. Zhuang, Y. Zhuang, J. E. Gonzalez, *et al.*, “Vicuna: An open-source chatbot impressing gpt-4 with 90%\* chatgpt quality,” See <https://vicuna.lmsys.org> (accessed 14 April 2023), 2023.
- [16] T. Dettmers, A. Pagnoni, A. Holtzman, and L. Zettlemoyer, “QLoRA: Efficient finetuning of quantized llms,” *arXiv preprint arXiv:2305.14314*, 2023.
- [17] Stability AI, “Stable Beluga.” <https://stability.ai/news/stable-beluga-large-instruction-fine-tuned-models>, 2023.
- [18] T. Dettmers and L. Zettlemoyer, “The case for 4-bit precision: k-bit inference scaling laws,” in *International Conference on Machine Learning*, pp. 7750–7774, PMLR, 2023.
- [19] Z. Yao, R. Yazdani Aminabadi, M. Zhang, X. Wu, C. Li, and Y. He, “Zeroquant: Efficient and affordable post-training quantization for large-scale transformers,” *Advances in Neural Information Processing Systems*, vol. 35, pp. 27168–27183, 2022.
- [20] S. Merity, C. Xiong, J. Bradbury, and R. Socher, “Pointer sentinel mixture models,” *arXiv preprint arXiv:1609.07843*, 2016.
- [21] A. Ahmadian, S. Dash, H. Chen, B. Venkitesh, S. Gou, P. Blunsom, A. Üstün, and S. Hooker, “Intriguing properties of quantization at scale,” *arXiv preprint arXiv:2305.19268*, 2023.
- [22] H. Touvron, L. Martin, K. Stone, P. Albert, A. Almahairi, Y. Babaei, N. Bashlykov, S. Batra, P. Bhargava, S. Bhosale, *et al.*, “Llama 2: Open foundation and fine-tuned chat models,” *arXiv preprint arXiv:2307.09288*, 2023.
- [23] Y. Bengio, N. Léonard, and A. Courville, “Estimating or propagating gradients through stochastic neurons for conditional computation,” *arXiv preprint arXiv:1308.3432*, 2013.
- [24] J. Choi, Z. Wang, S. Venkataramani, P. I.-J. Chuang, V. Srinivasan, and K. Gopalakrishnan, “Pact: Parameterized clipping activation for quantized neural networks,” *arXiv preprint arXiv:1805.06085*, 2018.
- [25] M. Nagel, M. Fournarakis, R. A. Amjad, Y. Bondarenko, M. Van Baalen, and T. Blankevoort, “A white paper on neural network quantization,” *arXiv preprint arXiv:2106.08295*, 2021.
- [26] A. Gholami, S. Kim, Z. Dong, Z. Yao, M. W. Mahoney, and K. Keutzer, “A survey of quantization methods for efficient neural network inference,” in *Low-Power Computer Vision*, pp. 291–326, Chapman and Hall/CRC, 2022.
- [27] B. Jacob, S. Kligys, B. Chen, M. Zhu, M. Tang, A. Howard, H. Adam, and D. Kalenichenko, “Quantization and training of neural networks for efficient integer-arithmetic-only inference,” in *Proceedings of the IEEE conference on computer vision and pattern recognition*, pp. 2704–2713, 2018.

- [28] M. Nagel, M. v. Baalen, T. Blankevoort, and M. Welling, “Data-free quantization through weight equalization and bias correction,” in *Proceedings of the IEEE/CVF International Conference on Computer Vision*, pp. 1325–1334, 2019.
- [29] M. Nagel, R. A. Amjad, M. Van Baalen, C. Louizos, and T. Blankevoort, “Up or down? adaptive rounding for post-training quantization,” in *International Conference on Machine Learning*, pp. 7197–7206, PMLR, 2020.
- [30] P. Wang, Q. Chen, X. He, and J. Cheng, “Towards accurate post-training network quantization via bit-split and stitching,” in *International Conference on Machine Learning*, pp. 9847–9856, PMLR, 2020.
- [31] I. Hubara, Y. Nahshan, Y. Hanani, R. Banner, and D. Soudry, “Accurate post training quantization with small calibration sets,” in *International Conference on Machine Learning*, pp. 4466–4475, PMLR, 2021.
- [32] Y. Li, R. Gong, X. Tan, Y. Yang, P. Hu, Q. Zhang, F. Yu, W. Wang, and S. Gu, “Breqq: Pushing the limit of post-training quantization by block reconstruction,” *arXiv preprint arXiv:2102.05426*, 2021.
- [33] Z. Deng, X. Wang, S. Sharify, and M. Orshansky, “Mixed-precision quantization with cross-layer dependencies,” *arXiv preprint arXiv:2307.05657*, 2023.
- [34] G. Park, B. Park, S. J. Kwon, B. Kim, Y. Lee, and D. Lee, “nuqmm: Quantized matmul for efficient inference of large-scale generative language models,” *arXiv preprint arXiv:2206.09557*, 2022.
- [35] T. Dettmers, R. Svirschevski, V. Egiazarian, D. Kuznedelev, E. Frantar, S. Ashkboos, A. Borzunov, T. Hoefler, and D. Alistarh, “SpQR: A sparse-quantized representation for near-lossless llm weight compression,” *arXiv preprint arXiv:2306.03078*, 2023.
- [36] C. Lee, J. Jin, T. Kim, H. Kim, and E. Park, “OWQ: Outlier-aware weight quantization for efficient fine-tuning and inference of large language models,” in *Proceedings of the AAAI Conference on Artificial Intelligence*, vol. 38, pp. 13355–13364, 2024.
- [37] J. Devlin, M.-W. Chang, K. Lee, and K. Toutanova, “BERT: Pre-training of deep bidirectional transformers for language understanding,” *arXiv preprint arXiv:1810.04805*, 2018.
- [38] M. Lewis, Y. Liu, N. Goyal, M. Ghazvininejad, A. Mohamed, O. Levy, V. Stoyanov, and L. Zettlemoyer, “BART: Denoising sequence-to-sequence pre-training for natural language generation, translation, and comprehension,” *arXiv preprint arXiv:1910.13461*, 2019.
- [39] J. Lee, M. Kim, S. Baek, S. Hwang, W. Sung, and J. Choi, “Enhancing computation efficiency in large language models through weight and activation quantization,” in *Proceedings of the 2023 Conference on Empirical Methods in Natural Language Processing*, pp. 14726–14739, 2023.
- [40] N. Trukhanov and I. Soloveychik, “Accurate block quantization in LLMs with outliers,” *arXiv preprint arXiv:2403.20137*, 2024.

## A Appendix

### A.1 Detailed Quantization Results of the OPT and llama2 Family w/ and w/o SmoothQuant

Tables 6 and 7 illustrate the perplexity of the OPT and llama2 family on WikiText-2-test, when quantized to various fixed-point and MX formats. Based on the experimental results of both families, we observe that: a) Aggressive quantization to small bit-widths significantly impairs model performance, whereas quantizing to higher bit-widths has a negligible effect on perplexity. b) Quantization results using different MXINT formats yield better perplexity compared to fixed-point formats with the same bit-width. c) Among MXINT formats with the same precision, enabling SmoothQuant is more advantageous when quantizing to formats with larger block sizes than to formats with smaller block sizes. d) SmoothQuant is effective with lower than 8-bit MXINT formats but not with 8-bit MXINT formats. e) Finally, for the studied models regardless of the quantization format and precision, the benefits of enabling SmoothQuant are marginal for larger models and higher quantization precisions, but notably pronounced for smaller models with more constrained bit-widths.

Table 6: Quantization results for the OPT models with different sizes on *WikiText-2-test*, with and without SmoothQuant. Act, Wgt, SQ, and PPL denote activation, weight, SmoothQuant, and perplexity, respectively. ↓: the lower the metric, the better the result. We used *per-tensor affine* quantization for the fixed-point formats. \*: The vocabulary size for *WikiText-2* is around 50000; a perplexity number larger than 50000 is most likely due to a numerical issue. LR: Likelihood Ratio of PPL with SmoothQuant enabled over PPL with SmoothQuant disabled.

Model Act & Wgt format	OPT-1.3B			OPT-6.7B			OPT-30B		
	↓PPL w/o SQ	↓PPL w/ SQ	LR	↓PPL w/o SQ	↓PPL w/ SQ	LR	↓PPL w/o SQ	↓PPL w/ SQ	LR
Baseline (FP16)	<b>14.63</b>	N/A	N/A	<b>10.86</b>	N/A	N/A	<b>9.56</b>	N/A	N/A
MXINT16-64	<b>14.63</b>	<b>14.62</b>	1.00	<b>10.86</b>	<b>10.86</b>	1.00	<b>9.56</b>	<b>9.56</b>	1.00
MXINT16-32	<b>14.62</b>	<b>14.62</b>	1.00	<b>10.86</b>	<b>10.86</b>	1.00	<b>9.56</b>	<b>9.56</b>	1.00
INT-8	16.48	15.44	1.07	15.01	11.17	1.34	315.83	9.79	32.26
MXINT8-128	17.21	<b>14.63</b>	1.18	<b>10.86</b>	<b>10.86</b>	1.00	<b>9.56</b>	<b>9.56</b>	1.00
MXINT8-64	14.81	<b>14.63</b>	1.01	<b>10.86</b>	<b>10.86</b>	1.00	<b>9.56</b>	<b>9.56</b>	1.00
MXINT8-32	14.64	<b>14.63</b>	1.00	<b>10.86</b>	<b>10.86</b>	1.00	9.57	<b>9.56</b>	1.00
MXINT8-16	<b>14.63</b>	<b>14.63</b>	1.00	10.87	<b>10.86</b>	1.00	9.58	<b>9.56</b>	1.00
INT-6	4421.20	291.79	15.15	12392.76	121.52	101.98	11415.95	1131.71	10.09
MXINT6-128	25.40	24.64	1.03	11.02	10.98	1.00	9.60	<b>9.52</b>	1.01
MXINT6-16	15.07	<b>14.92</b>	1.01	10.94	<b>10.90</b>	1.00	9.58	9.56	1.00
INT-4	83368.28	37182.13	2.24	13645.72	12064.92	1.13	34580.63	125530.61 <sup>+</sup>	0.28
MXINT4-128	2862.62	55.25	51.81	32.85	17.27	1.90	17.28	11.07	1.56
MXINT4-16	25.04	<b>22.76</b>	1.10	<b>13.82</b>	14.26	0.97	10.60	<b>10.47</b>	1.01

Table 7: Quantization results for the llama2-7B and llama2-13B models on *WikiText-2-test*, with and without SmoothQuant. Act, Wgt, SQ, and PPL denote activation, weight, SmoothQuant, and perplexity, respectively. ↓: the lower the metric, the better the result. We used *per-tensor affine* quantization for the fixed-point formats. LR: Likelihood Ratio of PPL with SmoothQuant enabled over PPL with SmoothQuant disabled.

Model Act & Wgt format	llama2-7B			llama2-13B		
	↓PPL w/o SQ	↓PPL w/ SQ	LR	↓PPL w/o SQ	↓PPL w/ SQ	LR
Baseline (FP16)	<b>5.11</b>	N/A	N/A	<b>4.57</b>	N/A	N/A
MXINT16-64	<b>5.11</b>	<b>5.11</b>	1.00	<b>4.57</b>	<b>4.57</b>	1.00
MXINT16-32	<b>5.11</b>	<b>5.11</b>	1.00	<b>4.57</b>	<b>4.57</b>	1.00
INT-8	237.40	498.39	0.48	186.04	61.65	3.02
MXINT8-128	5.13	<b>5.12</b>	1.00	4.58	4.58	1.00
MXINT8-64	<b>5.12</b>	<b>5.12</b>	1.00	4.58	4.58	1.00
MXINT8-32	<b>5.12</b>	<b>5.12</b>	1.00	4.58	<b>4.57</b>	1.00
MXINT8-16	<b>5.12</b>	<b>5.12</b>	1.00	<b>4.57</b>	<b>4.57</b>	1.00
INT-6	53068.17	52256.23	1.02	25028.43	39820.93	0.63
MXINT6-128	5.30	5.26	1.01	4.72	4.68	1.01
MXINT6-16	5.18	<b>5.16</b>	1.00	4.62	<b>4.61</b>	1.00
INT-4	45024.28	38934.63	1.16	140992.44	136368.02	1.03
MXINT4-128	39.15	25.49	1.54	23.52	13.73	1.71
MXINT4-16	7.01	<b>6.62</b>	1.06	6.21	<b>5.78</b>	1.07

## A.2 SmoothQuant and GPTQ Interaction for quantization of DistilGPT2 and the LLaMA family

**DistilGPT2.** To understand how SmoothQuant interacts with GPTQ when quantizing a small model like DistilGPT2, we quantized this model to INT-8 and MXINT4 using these two methods individually, as well as in combination. (Table 8). We found that the best results for both quantization formats are achieved when only the GPTQ method is applied.

Table 8: DistilGPT2 perplexity results on *WikiText-2-test*, with enabling/disabling GPTQ and A-W SmoothQuant. A, W, SQ, and PPL denote activation, weight, SmoothQuant, and perplexity, respectively. ↓: the lower the metric, the better the result. We used *per-tensor affine* quantization for the INT-8 format.

Act & Wgt format		A:INT-8 W:INT-8	A:MXINT8 W:MXINT4
GPTQ	A-W SQ	DistilGPT2 (FP32 ↓PPL: 46.07)	
disabled	disabled	59.23	72.97
disabled	enabled	60.57	72.93
enabled	disabled	<b>49.82</b>	<b>53.93</b>
enabled	enabled	52.12	56.65

**LLaMA and llama2 family.** We conducted a similar experiment for the LLaMA and llama2 families, demonstrating that for all studied models and quantization formats, except when quantizing llama2-13B to INT-8, the best results were obtained when only GPTQ was applied. For the latter case, SmoothQuant was necessary to improve the perplexity degradation of the quantized model (Table 9).

Table 9: Quantization results for the LLaMA and the llama2 families with different sizes on *WikiText-2-test*, with enabling/disabling GPTQ and A-W SmoothQuant. A, W, SQ, and PPL denote activation, weight, SmoothQuant, and perplexity, respectively. ↓: the lower the metric, the better the result. We used *per-tensor affine* quantization for the INT-8 format.

Act & Wgt format		A:INT-8 W:INT-8	A:MXINT8 W:MXINT4
GPTQ	SQ	LLaMA-7B (FP16 ↓PPL: 5.67)	
disabled	disabled	19.01	6.31
disabled	enabled	17.47	<b>6.18</b>
enabled	disabled	<b>17.44</b>	7.23
enabled	enabled	24.27	6.24
GPTQ	SQ	LLaMA-13B (FP16 ↓PPL: 5.09)	
disabled	disabled	28.90	5.43
disabled	enabled	32.86	5.47
enabled	disabled	<b>28.41</b>	<b>5.32</b>
enabled	enabled	31.82	5.37
GPTQ	SQ	LLaMA-30B (FP16 ↓PPL: 4.10)	
disabled	disabled	17.72	4.46
disabled	enabled	21.39	4.49
enabled	disabled	<b>17.39</b>	<b>4.37</b>
enabled	enabled	34.13	4.43
GPTQ	SQ	llama2-7B (FP16 ↓PPL: 5.11)	
disabled	disabled	237.40	5.56
disabled	enabled	303.96	5.61
enabled	disabled	<b>231.23</b>	<b>5.47</b>
enabled	enabled	239.88	5.50
GPTQ	SQ	llama2-13B (FP16 ↓PPL: 4.57)	
disabled	disabled	186.04	4.82
disabled	enabled	58.16	4.93
enabled	disabled	181.67	<b>4.76</b>
enabled	enabled	<b>48.61</b>	4.86

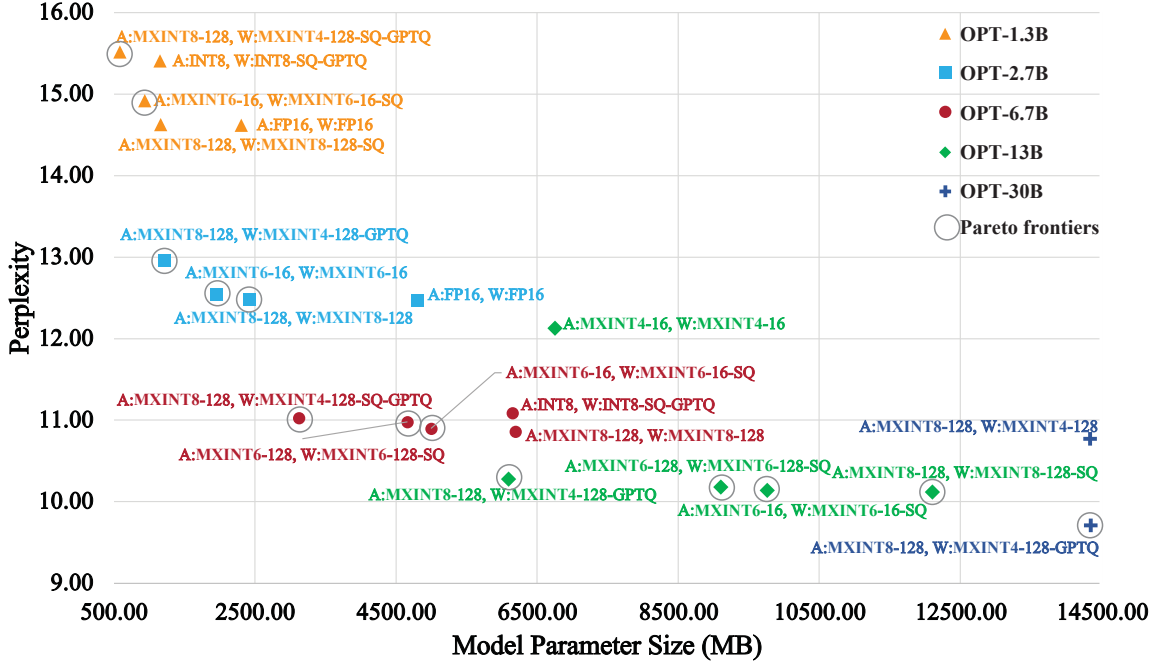


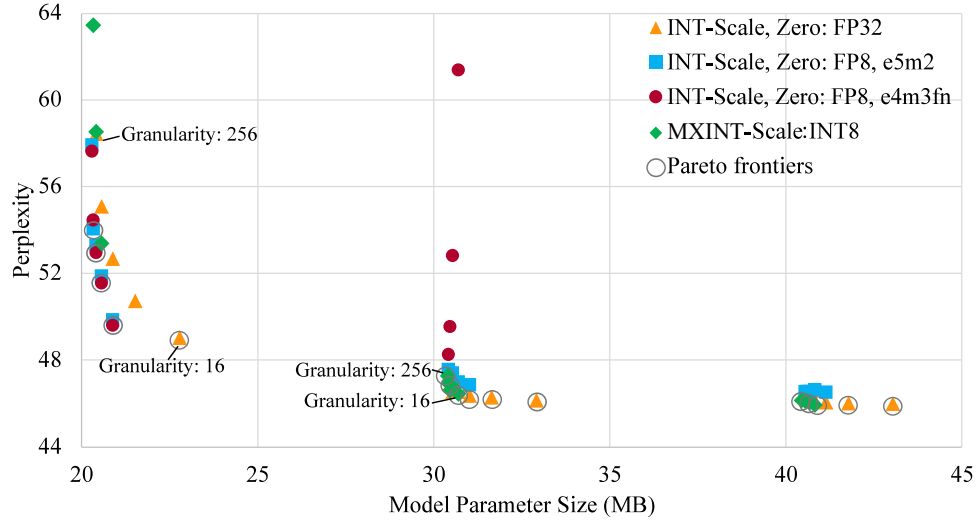
Figure 4: Perplexity for the OPT family with different sizes when quantized to INT-8, MXINT8, and MXINT4. The Y-axis represents perplexity. The X-axis represents model parameter size including the additional scale parameters required by the SmoothQuant quantization method. Note that the GPTQ algorithm does not introduce any additional model parameters during the inference. The *Per-tensor affine* scheme is used for INT-8 quantization of both activations and weights. *A*, *W*, and *SQ* denote activation, weight, and SmoothQuant, respectively. The points corresponding to the quantized models on Pareto frontiers are indicated by a gray circle.

### A.3 Pareto frontier study for the OPT family

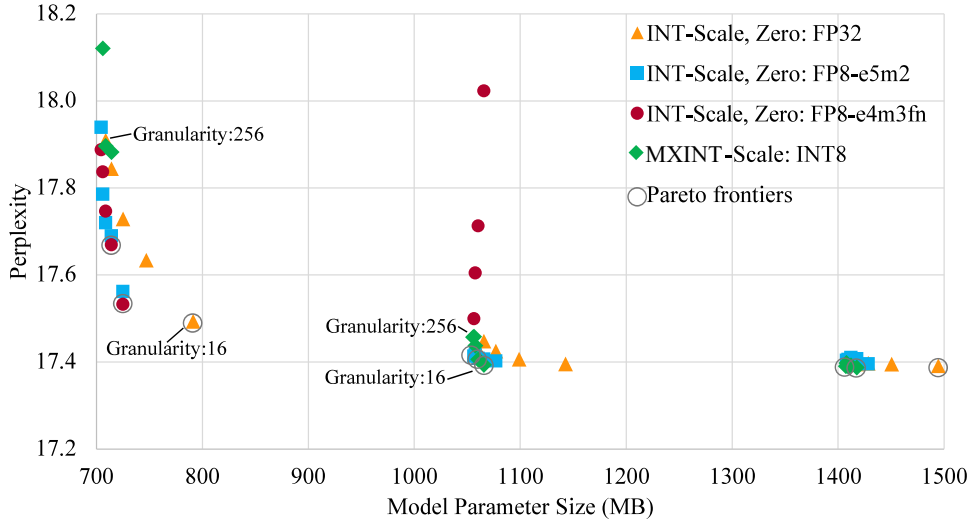
Figure 4 illustrates the perplexity of the OPT family on WikiText-2-test when quantized to different formats. Each point on the figure corresponds to a quantization configuration, indicating the activation and weight formats and whether SmoothQuant and GPTQ are enabled or disabled. The quantized models positioned on Pareto frontiers are marked with a gray circle. We observe that, generally, for medium and large-sized models (e.g., OPT-13B, and OPT-30B) with restrictive quantization to MXINT4, the points appearing on the Pareto frontiers are those with only GPTQ enabled. However, for smaller models (e.g., OPT-1.3B), both GPTQ and SQ should be applied jointly to effectively reduce perplexity when aggressively quantizing the models to MXINT4. For less restrictive quantization to MXINT6, only SmoothQuant is sufficient to mitigate perplexity degradation. Finally, with quantization to MXINT8, none of these techniques is required.

### A.4 Block size granularity effect on quantization

To study the effects of block size granularity on quantization to fixed-point and microscaling formats, we conducted a comprehensive study on DistilGPT2 and GPT-xl, the smallest and the largest networks from the GPT2 family. We considered quantization with block sizes of 16, 32, 64, 128, and 256 for both fixed-point and microscaling data formats. For each combination of format and granularity we evaluated perplexity of the models on WikiText-2 when quantized to 4, 6, and 8 bits (Figure 5). For integer formats, we applied an affine quantization scheme, incorporating zero points and scales in three different formats: *FP8-e5m2*, *FP8-e4m3fn*, and *FP32*. For MXINT, the scale data type is INT8, and zero point is not used. We found that (a) with extreme quantization to 4-bit (points on the left cluster), most points on the Pareto frontier align with INT8 quantization with zero points and scales in the *FP8-e4m3fn* format; additionally, for a quantization granularity of 16, the INT8 with *FP32* scale/zero point format also appears on the Pareto frontier, and (b) for quantization to 6-bit and 8-bit, the middle and right clusters, the majority of points on the Pareto frontier are associated with MX data-types. Notably, for DistilGPT2, points corresponding to INT8-*FP32* are also present on the Pareto frontiers when the quantization granularity is small (16 and 32).



(a) DistilGPT2



(b) GPT2-XL

Figure 5: Perplexity for (a) DistilGPT2 and (b) GPT2-XL when quantized to 8, 6, and 4 bit-widths with different quantization granularities. The Y-axis represents perplexity. The X-axis represents the model size in MB. The *affine* scheme is used for INT quantization of weights. The points corresponding to the quantized models on Pareto frontiers are indicated by a gray circle.